Journal of Applied Polymer Science

Preparation, Characterization, and Applicability of Novel Calix[4]arene-Based Cellulose Acetate Membranes in Gas Permeation

Sarah Farrukh,[1] Fozia T. Minhas,[2] Arshad Hussain,[1] Shahabuddin Memon,[2] M. I. Bhanger,[3] M. Mujahid[1]

[1]School of Chemical and Materials Engineering, National University of Sciences and Technology, H-12,44000, Islamabad, Pakistan

[2]National Centre of Excellence in Analytical Chemistry, University of Sindh, Jamshoro 76080, Pakistan

[3]HEJ Research Institute of Chemistry, University of Karachi, Karachi 75270, Pakistan

Correspondence to: F. T. Minhas (E-mail: tabasumfouzia@yahoo.com)

ABSTRACT: Cellulose acetate (CA) is well known glassy polymer used in the fabrication of gas-separation membranes. In this study, 5,11,17,23-tetrakis(*N*-morpholinomethyl)-25,26,27,28-tetrahydroxycalix[4]arene (CL) was blended with CA to study the gas-permeation behavior for CO_2, N_2, and CH_4 gases. We prepared the pure CA and CA/CL blended membranes by following a diffusion-induced phase-separation method. Three different concentrations of CL (3, 10, and 30 wt %) were selected for membrane preparation. The CA/CL blended membranes were then characterized via Fourier transform infrared (FTIR) spectroscopy, scanning electron microscopy (SEM), atomic force microscopy (AFM), and X-ray diffraction analysis. The homogeneous blending of CL and CA was confirmed in the CA/CL blended membranes by both SEM and AFM analysis. In addition to this, the surface roughness of the CA/CL blended membranes also increased with increasing CL concentration. FTIR analysis described the structural modification in the CA polymer after it was blended with CL too. Furthermore, CL improved the tensile strength of the CA membrane appreciably from 0.160 to 1.28 MPa, but this trend was not linear with the increase in the CL concentration. CO_2, CH_4, and N_2 gases were used for gas-permeation experiments at 4 bars. With the permeation experiments, we concluded that permeability of N_2 was higher in comparison to those of CO_2 and CH_4 through the CA/CL blended membranes. © 2013 Wiley Periodicals, Inc. J. Appl. Polym. Sci. **2014**, *131*, 39985.

KEYWORDS: blends; cellulose and other wood products; membranes; oil and gas; properties and characterization

Received 24 May 2013; accepted 18 September 2013

DOI: 10.1002/app.39985

INTRODUCTION

Membrane-separation technology has evolved as a rapidly growing field during the past few decades, and it has been approved economically and technically as a favorable and competent separation process compared to the other separation techniques in use[1–5] because membrane technology offers numerous advantages over other technologies, including a low energy requirement, smaller footprint, low capital and operation costs, environmental friendliness,[6–10] and flexibility in handling at a higher flow rate, pressure, and various feed compositions. Membrane gas separation, a relatively young technology, has emerged in the last 15 years to successfully compete with other well-established industrial gas-separation processes, such as cryogenic distillation, absorption, and pressure swing adsorption.[11] Commercially, the most widely practiced separations using membranes include the separation of O_2 and N_2; the recovery of H_2 from mixtures with larger components such as N_2, CH_4, and CO_2; and the removal of CO_2 from natural gas mixtures.[12]

In many applications, polymeric membranes are used because of their processing feasibility and cost. The gas permeation through polymeric material is influenced by the polarity and structural characteristics of the polymer and permeate gas. The structural regularity and compactness in polymeric material increases the gas selectivity while reducing the permeability. On the other hand, bulky substituent groups on either the main chain or side chain of the polymer result in spaces throughout the whole polymer matrix; this increases the gaseous permeability. Thus, according to Robeson's view for polymeric membranes, a tradeoff exits between the gas permeability and selectivity.[13] Therefore, many efforts have focused on improving the polymer characteristics either by blending with other polymers or through using various inorganic additives.

In this context, cellulose acetate (CA) was selected as a polymeric material in this study to fabricate membranes for gaseous separation because of its unproblematic availability, low cost, good strength, and ease of handling.[14] To this point, the gas-separation efficiency of CA has been increased in different ways by the introduction of zeolites,[15] transition-metal complexes,[16] and silicon species[17] into its matrix. Furthermore, poly(methyl methacrylate),[18] poly(ethylene glycol),[19] and Si[20] were also incorporated into the cellulose polymer to prepare a polymeric membrane of comparable efficiency. A CA membranes are also used in facilitated transport by the inclusion of an aqueous carbonate solution.[21] However, much work is still needed to make CA membranes with particular properties.

Recently, prime importance has been attributed toward calixarenes, which are supramolecular receptors for ionic and neutral species. Calixarene exhibits a central cavity surrounded by upper *p-tert* butyl and lower —OH rims. Both rims are capable of functionalization, and therefore, a variety of calixarene derivatives has been synthesized for specific applications up to this point.[22] Hence, the complexation of calixarene with a particular target follows host–guest relationship because of the cavity along with functionalized rims. Therefore, it is successfully applied in metal complexation,[23] liquid membranes,[24,25] and potentiometric and optical systems.[26] Furthermore, the use of calixarene as an adsorbent for volatile guests, such as CH_4, CF_4, CF_3Br, and CO_2, is a new advancement.[27–29] Previously, it was believed that gases flowed around the calixarene crystal without interacting with them. However, in many new investigations, calixarene has appeared as a promising material for the absorption of CO_2 and CH_4 from gaseous mixtures. CO_2 and CH_4 uptake under standard temperature and pressure conditions is much greater in comparison to many porous materials in use today. It has been established that on average, two calixarene molecules facing each other in an offset arrangement generates an hourglass-shaped lattice void. In this particular arrangement, the host–guest ratio for CO_2 is 2:1, and for CH_4, it is 1:1.[30,31] Although the exact interaction mechanism of seemingly nonporous calixarene with CO_2 and CH_4 is still under investigation and it needs more conclusive experiments,[32,33] in addition to this, calixarenes are also used as carriers in various polymer inclusion membranes based on cellulose triacetate polymers for aqueous applications that show the considerable compatibility of calixarene with CA.[34–41]

With all of the previously discussed facts in mind, in this study, we planned to prepare calixarene-based CA membranes and to investigate their permeation behavior toward gases. This study opened up methods for the facile structural modification in the CA polymeric matrix with different economical calixarene derivatives. In addition to this, the remarkable inclusion ability of calixarene for volatile gases was also explored to examine the overall impact on gaseous permeation. For this purpose, 5,11,17,23-tetrakis(*N*-morpholinomethyl)-25,26,27,28-tetrahydroxycalix[4]arene (CL; as shown in Figure 1) was selected as a calixarene derivative; its preparation procedure was reported previously.[42] A diffusion-induced phase-separation (DIPS) method was followed to make CA/CL blended membranes of different concentrations (3, 10, and 30 wt %). The blended membranes were characterized with several analytical methods, including Fourier transform infrared

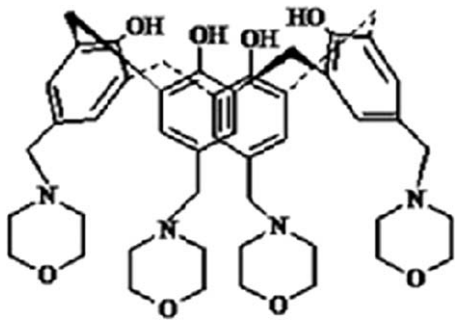

Figure 1. *p*-Morpholinomethylcalix[4]arene.

(FTIR) spectroscopy, scanning electron microscopy (SEM), atomic force microscopy (AFM), and X-ray diffraction (XRD) analysis. N_2, CO_2, and CH_4 gases were chosen for the permeation experiments of the CA/CL blended membranes to examine the specific host–guest interaction of CL with CO_2 and CH_4. The permeability of N_2 through these blended membranes was high compared to CO_2 and CH_4. The preparation of the CA/CL blended membranes and their gas-permeation properties are reported here for the first time.

EXPERIMENTAL

Materials

CA (Sigma Aldrich, Munich, Germany), with a degree of acetylation of 1.2, was used as membrane-forming material. Acetone (BDH Laboratory, London) was used as solvent to dissolve CA. Magnesium perchlorate (Sigma Aldrich, Munich, Germany) was used as a desiccant. Hexane (Merck, Darmstadt, Germany) was used to dry the membranes. All of these chemicals were bought from Shalimar Scientific Stores (Rawalpindi, Pakistan) and were used without further purification. Pure feed gases were bought from New Light Corp. (Pakistan).

Fabrication of the CA/CL Membranes

CL was prepared according to the reported procedure.[42] For the CA/CL membranes, 65 wt % dry acetone (with the addition of 10 wt % magnesium perchlorate) was mixed with 25 wt % CA with constant stirring. Different proportions of CL were sonicated and added to the CA mixture along with stirring. The blended mixture was kept for 2 h to remove bubbles after 24 h of stirring. The resulting casting solution was cast on a glass plate, placed in air for 20 s to evaporate the solvent, and gelled in ice–water for 20 min to complete the phase-separation process. The cast membrane was dipped in water at 80°C to separate the membrane from the glass surface. For drying purposes, the fabricated membrane underwent the solvent-exchange method. The CA/CL membrane was ready after it was heated at 60°C for 2 h. Three different concentrations of CL, that is, 3, 10, and 30 wt %, were blended with CA, apart from the synthesis of pure CA membrane, and these are referred to as M(b), M(c), M(d), and M(a), respectively.

MEMBRANE CHARACTERIZATION

SEM

The cross-sectional images of the membranes were obtained from SEM (JSM 6409A, JEOL, Japan) after sputter coating with

a thin gold film and then attached on brass plates with double-sided tape.

AFM

The root mean square values of the surface roughness of the membranes were measured by AFM. The pure and blended membranes were heated to remove moisture and then mounted on slab with double-sided tape. The slab containing membranes were placed in a JSPM-5200 (Japan) to get the surface images.

FTIR Spectroscopy

FTIR spectroscopy (FTIR Spectrum 100 PerkinElmer, MID IR) was used to obtain the qualitative structural analysis of the pure and CA/CL blended membrane with 1-cm^{-1} resolution in transmission mode with wave numbers from 450 to 4000 cm^{-1}. The small portion of the pure and CA/CL blended membranes were cut in circular shapes and placed in a pallet holder. The holder was then mounted in an FTIR instrument (PerkinElmer). All of the spectra (subtracted from the background spectra) were recorded at room temperature.

XRD

The XRD analysis was performed with an STOE Germany Theta–Theta diffractometer (Germany, software, WinXPoe X'Pert High Score) with Cu Kα monochromatic radiations (wavelength = 1.54 Å) at a scanning range of 13 to 32° with a step size of 0.05° and a step time of 1 s. The accelerating voltage was 30 kW, and the tube current was 20 mA.

Tensile Strength

The tensile strengths of the pure and CA/CL blended membranes were measured at room temperature with a Shimadzu universal testing machine (AG-XD Plus, Japan). The membranes were cut into a dumbbell shape with a gauge length of 50 mm and a width of 13 mm. The samples were clamped between two aluminum holders. One holder was attached to the lower base of UTM, and the other holder was attached with a force sensor. The time required for the mounting and testing of all samples was kept constant. Three samples of each membrane were tested to eliminate random error.

Permeation Experiments

The gas-permeation study of all of the fabricated CA/CL blended membranes was accomplished with the experimental setup given in Figure 2. Single gas-permeation experiments were conducted at 28°C with a pressure difference of 400 KPa. The setup was placed in a temperature-controlled chamber. Air circulation was also done to maintain the temperature and prevent condensation of water in the membrane module.

The basic principle of gas permeation through dense membranes was a solution-diffusion mechanism.[43] Gas permeation took place because of the pressure gradient across the membrane. The flow rates and pressures (feed and permeate) were measured by flow meters and pressure sensors, respectively. The permeability (P_i) of the CO_2, CH_4, and N_2 gases were calculated with eq. (1), derived from Fick's law of diffusion:

$$P_i = \frac{\dot{n}l}{P_2\text{-}P_1} \quad (1)$$

where $\dot{n}_i$ is the steady state flux of i feed gas [mol (STP)/m^2 s], l is the membrane thickness (m), and P_1 and P_2 are the pressures of the permeate and feed side, respectively (Pa).

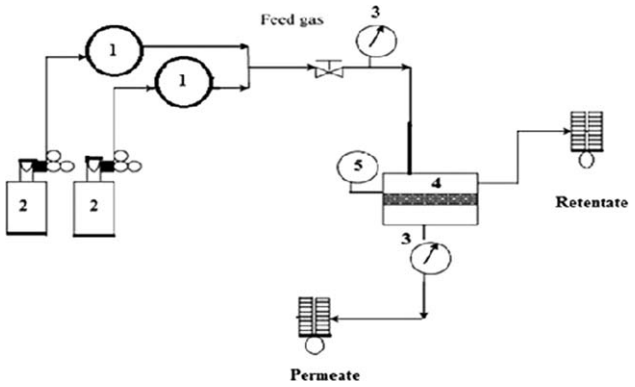

Figure 2. Schematic representation of the experimental setup: (1) flow meters, (2) gas cylinders, (3) pressure gauges, (4) membrane module, and (5) pressure sensor.

RESULTS AND DISCUSSION

DIPS Process

The DIPS technique was used to synthesize CA/CL blended membranes.[44] The cast membranes were placed in air to evaporate the solvent and then immersed in distilled water. The demixing of the solvent and nonsolvent (acetone–water) took place at this point. CA started to precipitate, and the diffusional mass exchange caused changes in the confined composition of the polymer membranes. The CA chains were repelled because of their low miscibility with water. These chains intertwined and gelled to form dense structure. After gelling, the dipping of the CA/CL membranes at 80°C in distilled water caused the destruction of the microporous structure and converted these in a nonporous structure. A number of parameters, such as the rate of solvent and nonsolvent exchange, temperature, relative humidity, and time delay in the immersion of the membrane in the nonsolvent, influenced the membrane morphology.[45]

FTIR Analysis

The role of spectroscopic analysis is crucial in polymer characterization. The surface characterization of membranes was done with IR spectroscopy to examine the molecular structure of the membranes. The FTIR spectra of the pure CA and CA/CL blended membranes are collectively presented in Figure 3. The FTIR spectrum of the pure CA membrane was compared with that of the CA/CL blended membranes. In the spectrum of pure CA, the peak at 3417 cm^{-1} was attributed to the stretching vibration of the carboxylic acid group (—COOH). The strong peak around 1790 cm^{-1} was assigned to the stretching mode of the C═O bond, and another peak at 1370 cm^{-1} showed the bending of the C—CH_3 group. The characteristic peak around 1235 cm^{-1} was attributed to the asymmetric stretching of the ether C—O—C vibration. However, in the FTIR spectrum of CL, a distinctive peak was indicated at 1454 cm^{-1} for the C—N stretching vibrations and was followed by a band at 1107 cm^{-1}, which showed the stretching vibrations of C—O. The FTIR spectrum of the CA/CL blended membrane indicated slight changes in the peaks associated with the carbonyl (C═O) and

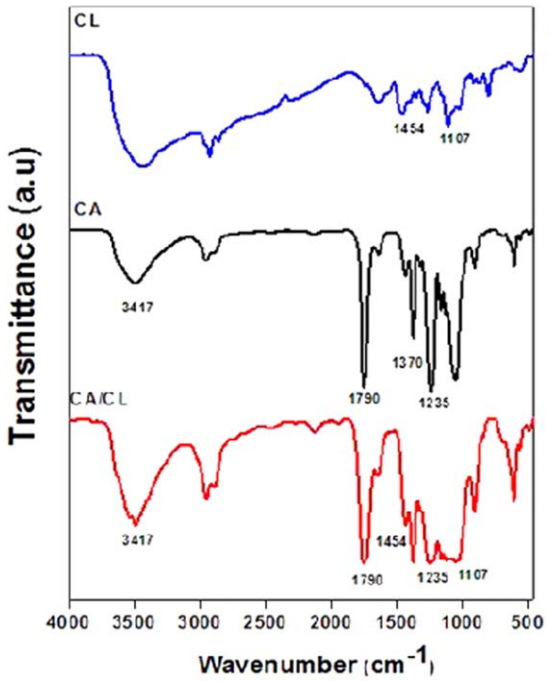

Figure 3. FTIR spectra of the CL, CA, and CA/CL blended membranes. [Color figure can be viewed in the online issue, which is available at wileyonlinelibrary.com.]

carboxylic acid group (—COOH) in comparison to FTIR spectrum of the pure CA. Both of the bands in the FTIR spectrum of the CA/CL blended membrane stretched toward lower frequency and confirmed interaction between CA and CL. So, we concluded that the CL interacted successfully with the polymer in the CA/CL blended membranes.

SEM Analysis

The surface morphologies of the pure CA and CA/CL blended membranes with various concentrations were examined by SEM. Figure 4 depicts the comparison of the SEM images of both the pure and CA/CL blended membranes at 5000 and 10,000× magnifications. The SEM image of the pure CA membrane showed a dense, smooth, and nonporous structure. However, the CA/CL blended membranes with different concentrations (3, 10, and 30 wt %) revealed appealing results. The SEM images of all of the blended membranes at both magnifications were dense but with some granular appearance. This observation clearly confirmed the homogeneous dispersion of CL into the CA matrix and, consequently, effective bonding between them. These results were also supported by the previously described FTIR results.

AFM Analysis

AFM is a well-recognized and discriminative tool for the surface topography analysis of membranes. Therefore, the influence of the CL additive on the pure CA membranes was examined under AFM in tapping mode. Three-dimensional AFM images of the top surfaces of all of the membranes with scanning area of 5 × 5 μm^2 are presented in Figure 5. The surface roughness parameters, the arithmetic mean roughness (R_a) and the square average roughness (R_q), for all of the membranes were gathered

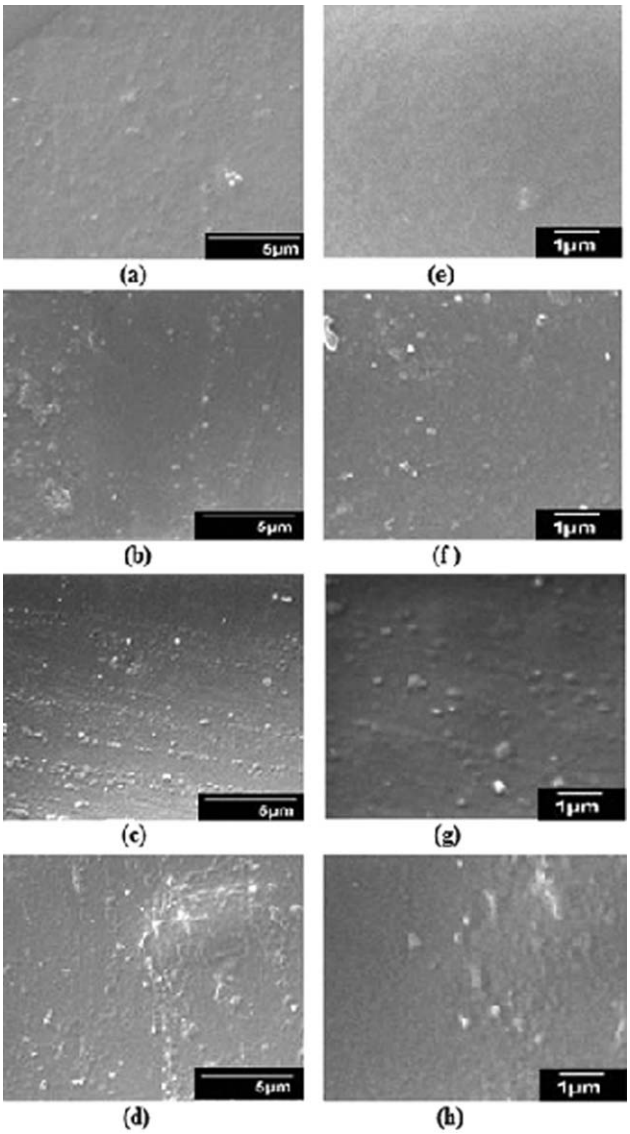

Figure 4. SEM views of the (a,e) CA, (b,f) CA–3 wt % CL, (c,g) CA–10 wt % CL, and (d,h) CA–30 wt % CL membranes at 5000 and 10,000× magnifications.

by AFM analysis software and are combined in Table I. The light regions in the AFM images correspond to height, whereas the dark regions denote depression. The AFM results were consistent with the SEM findings. From the results, we inferred that the incorporation of CL at various concentrations somehow increased the surface roughness with respect to the pure CA membrane except at the 3 wt % CL concentration. The obvious interpretation for this behavior was the existence of CL in the CA matrix, which spread homogeneously but generated somewhat heightened features.

XRD Analysis

The structural features of polymer were mostly investigated by XRD. It is a well-known and frequently applied technique for examining the crystallinity and amorphous phases of membranes. In the XRD spectrum, the peak position, peak width, and peak height are determining parameters in the analysis of

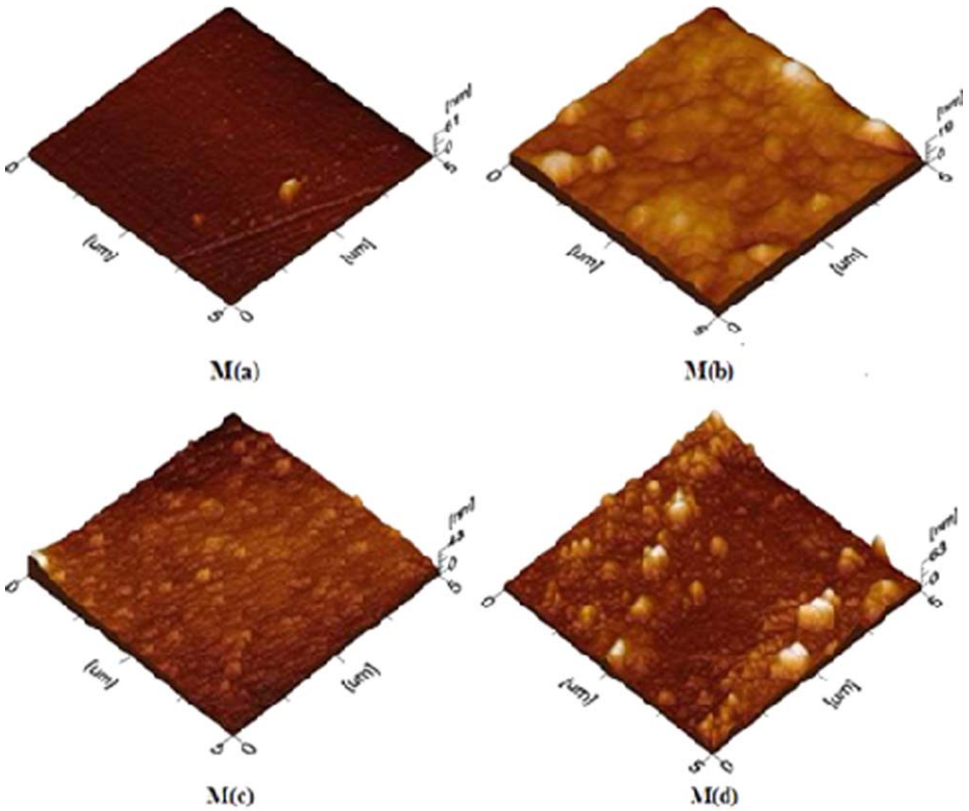

Figure 5. AFM scans of the CA, CA–3 wt % CL, CA–10 wt % CL, and CA–30 wt % CL membranes [M(a), M(b), M(c), and M(d), respectively]. [Color figure can be viewed in the online issue, which is available at wileyonlinelibrary.com.]

the structure of typical solids. The XRD study of the pure CA and CA/CL blended membranes was carried out, and the results are displayed in Figure 6. The ordered pattern in any polymer creates crystallinity, whereas the reverse is true for the amorphous part. Sharp peaks with a high intensity ensure crystallinity, and wide peaks with a low intensity indicate the amorphous part of the polymer. CA is usually considered a semicrystalline polymer, and pure CA exhibits a diffuse peak at a 2θ of 23 with maximum intensity. The reason for the low crystallinity in CA is hydrogen bonding between acetyl and hydroxyl groups. However, as shown in Figure 6, the XRD peaks in the CA/CL blended membrane were not sharp enough relevant to pure CA, and they appeared at a low position. The possible explanation for this behavior was the successful dispersion of CL into the CA matrix because the CL content disrupted the aforementioned interaction between acetyl and hydroxyl groups by estab-

Table I. Mean Roughness Values of the Fabricated Membranes

Fabricated membrane	R_q (nm)	R_a (nm)
M(a)	3.45 ± 0.10	2.41 ± 0.28
M(b)	1.84 ± 0.56	1.35 ± 0.36
M(c)	4.59 ± 0.34	3.52 ± 0.63
M(d)	8.47 ± 0.88	6.26 ± 0.51

We calculated the errors by taking the standard deviation of three samples.

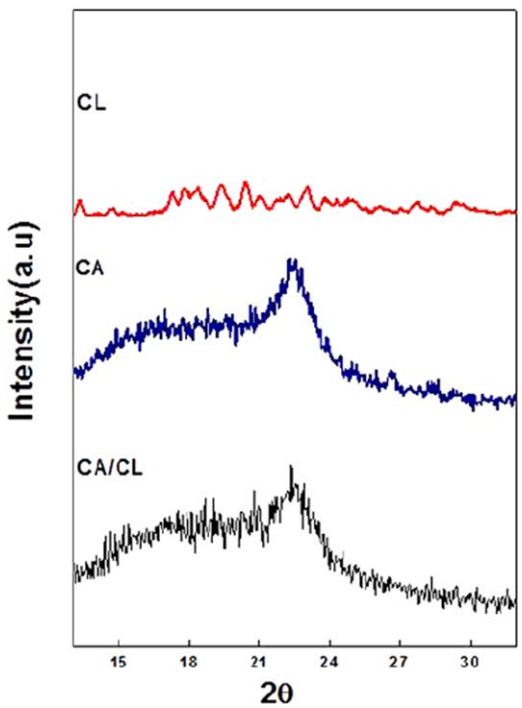

Figure 6. XRD spectra of the CL, CA, and CA/CL blended membranes. [Color figure can be viewed in the online issue, which is available at wileyonlinelibrary.com.]

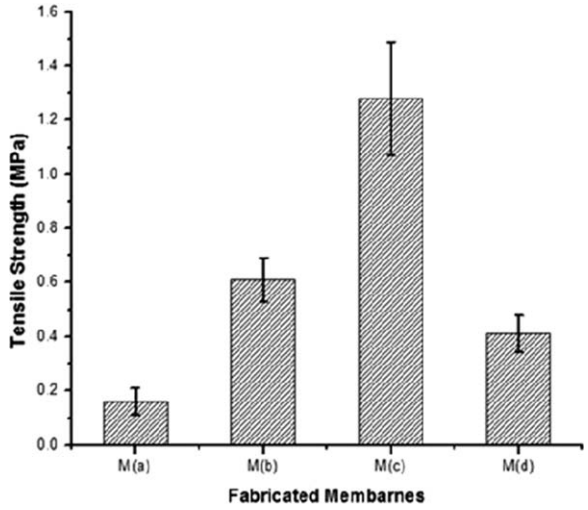

Figure 7. Tensile strength bar graph of the pure CA and CA/CL blended membranes.

lishing new linkages with them and thus lowered the crystallinity in the CA/CL blended membrane.

Tensile Strength Measurement

Figure 7 depicts the mechanical behavior of the pure and CA/CL blended membranes. The pure CA membrane was fragile and broke easily. From the results, it was obvious that CL addition in CA enhanced its mechanical strength, and the successful blending of both was proven. A very interesting result was observed for the CA/10 wt % CL blended membrane. The tensile strength increased and reached 1.28 MPa. The further addition of 30 wt % CL in the CA membrane caused a decrease in the tensile strength, but it was still better than the pure CA membrane. This phenomenon could be explained by the SEM images taken after tensile strength measurement.

The SEM micrographs (as shown in Figure 8) revealed that the CA membrane showed brittle behavior as expected because it was a glassy polymer. The degree of acetylation was the key factor in the strength of the CA membrane. The degree of acetylation was the extent to which the hydroxyl groups were acetylated in CA. It ranged from 0 (cellulose) to 3 (cellulose triacetate).[46] The acetyl groups in CA minimized the intermolecular hydrogen bonding, which caused flexibility in the polymer's chains.[47] The lower interaction between hydroxyl groups allowed the polymeric chains to move freely. The flexibility in polymeric chains resulted in an increase in the tensile strength.[48] In this study, the CA membrane had a low degree of acetylation (1.2). The acetyl groups were fewer compared to hydroxyl groups, which interacted more with each other and reduced the movement of polymeric membranes; therefore, the membranes exhibited a lower tensile strength value, which was 0.160 MPa. However, the blending of CA with CL [M(b) and M(c)] augmented the tensile strength. This was probably due to the interaction between the polymer and CL, which enhanced the polymeric chain mobility and increased the flexibility.[49] Therefore, M(b), with 3 wt % CL blending, showed a lower increment in the tensile strength with increasing concentration (10 wt %) of CL than M(c), which represented a very high tensile strength. This fact was also supported by the dense morphology of both the M(a) and M(b) membranes in the SEM images (Figure 8) because of the low amount of CL (3 wt %) in

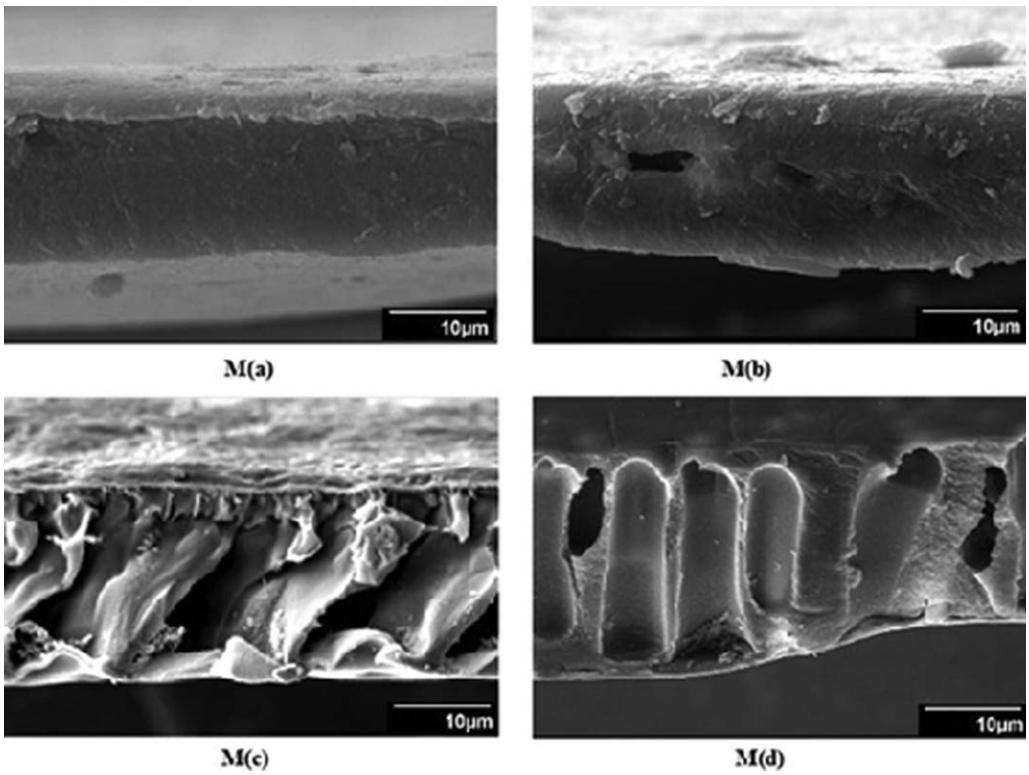

Figure 8. SEM cross sections of the CA/CL blended membranes after tensile strength testing.

Table II. Thickness of the Blended Membranes

Fabricated membrane	Thickness (μm)
M(a)	110 ± 0. 05
M(b)	154 ± 0.06
M(c)	209 ± 0.14
M(d)	287 ± 0.10

We calculated the errors by taking standard deviation of three samples.

CA in the M(b) membrane. However, it was more pronounced in M(c), with a high (10 wt %) CL content. Therefore, the SEM image of M(c) clearly revealed a change in the CA structure due to the presence and possible interaction between CL and CA. Conversely, the tensile strength of M(d) was low for two main reasons. First, a high CL concentration caused particle agglomeration and caused them not to disperse properly; this reduced the membrane's elasticity. Second, a high concentration of CL generated voids in the CA/CL membrane, which provided the active site for the membrane to fracture at a lower applied force.[50] This caused a decrement in the tensile strength.

The thickness of the membrane also affected the membrane characteristics and the mechanical strength and, therefore, the thickness; a comparison of the pure and CA/CL blended membranes is shown in Table II.

Gas-Permeation Experiments

The pure and CA/CL blended flat membranes were cut in a circular shape with a 4.5-cm radius and placed in a membrane cell. The membrane cell was evacuated for 4 h before experimentation. The cylinder of particular gas was connected with the membrane cell through a flow meter and pressure gauge. Another flow meter and pressure gauge were connected at the permeate side. The results of the gas permeability experiments are given in Figure 9 and Table III.

According to the results, the nitrogen gas was more permeable through the CA/CL blended membranes than the CO_2 and CH_4 gases. In the pure CA membrane, the permeability of N_2 was negligible with respect to the blended membranes. In the CA/30 wt % CL membrane, the permeability of N_2 gas decreased but was still better than that of the pure CA membrane. The CO_2 permeability of the pure CA membrane was high compared to those in all of the CA/CL blended membranes. However, when we compared the CA/CL blended membranes with different

Table III. Permeability Data of CO_2, CH_4, and N_2 Gases through the Pure and Blended Membranes

Fabricated membrane	$P(CH_4) \times 10^3$	$P(CO_2) \times 10^3$	$P(N_2) \times 10^3$
M(a)	0.581	0.830	0.232
M(b)	0.298	0.373	1.660
M(c)	0.199	0.456	1.751
M(d)	0.166	0.680	0.996

Permeability units = Barrer. 1 Barrer = 3.4×10^{-16} mol m m^{-2} s^{-1} Pa^{-1}.

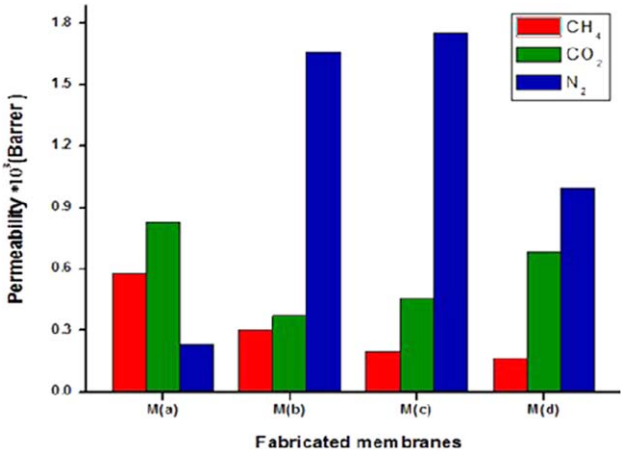

Figure 9. Permeability graph of CO_2, N_2, and CH_4 gases via the fabricated membranes. [Color figure can be viewed in the online issue, which is available at wileyonlinelibrary.com.]

concentrations, we observed that at high CL concentration, the CO_2 permeability increased but still was lower than that of the pure CA membrane. Although the CH_4 permeability trend of the CA/CL membranes was particularly different from the other gases, all of the CA/CL membranes exhibited a lower CH_4 permeability than the pure CA membrane.

The gas-permeation results of the CA/CL membranes were quite interesting. Generally, it is known that the diffusivity of gases has an inverse relationship to their kinetic diameters.[21,51] However, in this study, a distinctive trend was observed. A comparison of the kinetic diameters of all three gases is presented in Table IV. Despite its small kinetic diameter, CO_2 diffused through the CA/CL membrane more slowly than N_2, which has a relatively larger kinetic diameter. However, the permeation behavior of CH_4 through the CA/CL membrane was in accordance to its kinetic diameter. The possible explanation for this unique CO_2 permeation could have been the specific host–guest interaction between CL and CO_2. These experimental findings were also supported by previously published results, in which calixarene crystals selectively absorbed CO_2 among N_2, O_2, and air. It was proposed in these articles that two calixarene molecules form a lattice void suitable for CO_2 and CH_4 capture by arranging themselves face to face in an offset manner to give an hourglass-shaped appearance. However, the ratio of host to guest for CO_2 was 2:1, whereas it was 1:1 for CH_4, depending on their molecular dimensions, which fit them into a calixarene lattice void.[27–31] Thus, CL in the CA/CL blended membranes exhibited a remarkable molecular recognition for CO_2 and CH_4. Therefore, more N_2 permeated through these membranes relative to CO_2 and CH_4 because, at a high CL concentration, the

Table IV. Kinetic Diameters of the Gases[51]

Gas	Kinetic diameter (Å)
Nitrogen	3.6
Carbon dioxide	3.3
Methane	3.8

Table V. Performance of the CA-Based Membranes

Membrane	$P(CO_2) \times 10^3$	$P(CH_4) \times 10^3$	$P(N_2) \times 10^3$	Reference
Ethyl cellulose	0.120	0.011	-	17
Ethyl cellulose Si—$(OC_2H_5)_4$	0.225	0.029	-	17
CA + 10%PEG200	0.004	0.001	0.00091	19
CA + 10% PEG2000	0.006	0.0005	0.00045	19
CA + PPO + PEO + Si	0.012	0.0006	0.00041	20
CA + PPO + Si	0.010	0.0005	0.00036	20
CA + 2NKHCO$_3$ + 0.5*N* $NaAsO_2$	2.000	-	-	21
CA + CL	0.456	0.199	1.751	This study

Units of permeability = Barrer. 1 Barrer = 3.4×10^{-16} mol m m^{-2} s^{-1} Pa^{-1}.
Abbreviations: PEG2000: polyethylene glycol 2000, PPO: polypropylene oxide, PEO: polyethylene oxide.

opposite trend was observed for both N_2 and CO_2. Possibly, this indicated that at this high concentration, the number of unique lattice voids decreased because of the accumulation of CL molecules. Conclusively, the CA matrix proved sufficiently compatible with CL to explore its distinguishing recognition abilities toward CO_2 and CH_4. This work was at a preliminary level, and more experiments are needed to fully grasp the blending chemistry of calixarene derivatives in the CA matrix and their performance.

Comparison Study

A comparison of the CO_2, N_2, and CH_4 permeability of the CA/CL blended membrane and CA-based membranes is given in Table V. In a previously reported work, the permeability of gases was low, particularly that of N_2 gas. In contrast, the permeabilities of CO_2, N_2, and CH_4 through our novel CA/CL membranes were high. This was due to the presence of bulky substituent CL in the CA polymeric matrix, which resulted in the movement of polymeric chains to enhance the gas permeability.[52]

CONCLUSIONS

In this article, we described the novel, successful fabrication of CA/CL blended membranes and their utilization in a gas-permeation field for the first time. A calix[4]arene derivative (CL) was homogeneously mixed into the CA matrix to make a dense membrane. The concentration of CL was varied at 3, 10, and 30 wt % with respect to CA. The resulting membranes were analyzed by FTIR spectroscopy, SEM, AFM, and XRD analysis. Comparison of the FTIR spectra of the pure CL and CA with the CA/CL dense membrane clearly demonstrated proper interaction between them. SEM of all of the membranes revealed a nonporous, smooth, and dense surface layer. These results were also supported by AFM spectroscopy. The tensile strength measurement provided interesting observations. The addition of CL augmented the strength of the CA membrane. However, it dropped at a 30 wt % CL concentration. The gas permeation was also examined. The permeability of N_2 was pronounced compared to those of CO_2 and CH_4. A possible explanation for this fact was the unique interaction of CL with CO_2 and CH_4, in contrast to that with N_2, which created a difference in their permeation. This study drew paramount attention to the fact that calixarene derivatives of a particular functionality for a specific gas can be synthesized and successfully incorporated into the CA matrix. This CA–calixarene combination allowed us to improve the membrane strength along with the desired permeabilities.

ACKNOWLEDGMENTS

This work was supported by School of Chemical and Materials Engineering, National University of Sciences and Technology, Islamabad, Pakistan. The authors also thank the National Centre of Excellence in Analytical Chemistry, University of Sindh, Jamshoro.

REFERENCES

1. Peters, L.; Hussain, A.; Follmann, M.; Melin, T.; Hägg, M.-B. *Chem. Eng. J.* **2011**, *172*, 952.
2. Franco. J. A.; deMontigny, D.; Kentish, S. E.; Perera, J. M.; Stevens, G. F. *Chem. Eng. Sci.* **2009**, *64*, 4016.
3. Mofarahi, M.; Khojasteh, Y.; Khaledi, H.; Farahnak, A. *Energy* **2008**, *33*, 1311.
4. Yeo, Z. Y.; Chew, T. L.; Zhu, P. W.; Mohamed, A. R.; Chai, S.-P. *J. Nat. Gas Chem.* **2012**, *21*, 282.
5. Kebiche-Senhadji, O.; Bey, S.; Clarizia, G.; Mansouri, L.; Benamor, M. *Sep. Purif. Technol.* **2011**, *80*, 38.
6. Berry, R. I. *Chem. Eng.* **1981**, *88*, 63.
7. Spillman, R. W.; Sherwin, M. B. *Chem. Technol.* **1990**, *20*, 378.
8. Stern, S. A. *J. Membr. Sci.* **1994**, *94*, 1.
9. Mulder, M. Basic Principles of Membrane Technology, 2nd ed.; Kluwer Academic: Dordrecth, The Netherlands, **1996**.
10. Strathman, H. *J. Membr. Sci.* **1981**, *9*, 121.
11. Stern, S. A.; Bhide, B. D. *J. Membr. Sci.* **1993**, *81*, 209.
12. Noble, R. D. Membrane Separation Technology: Principles and Applications; Elsevier: Amsterdam, **1995**.
13. Robeson, L. M. *J. Membr. Sci.* **1991**, *62*, 165.
14. Chung, T. S.; Jiang, L. Y.; Li, Y. *Prog. Polym. Sci.* **2007**, *32*, 483.

15. Duval, J. M.; Kemperman, A. J. B.; Folkers, B.; Mulder, M. H. V.; Desgrandchamps, G.; Smolders, J. *Appl. Polym. Sci.* **1994**, *54*, 409.
16. Lee, K.-I.; Shim, I.-W.; Hwang, S.-T. *J. Membr. Sci.* **1991**, *60*, 207.
17. Li, G. S. U.S. Pat. 4,428,776 (**1984**).
18. Bikson, B.; Nelson, J. K.; Muruganadam, N. *J. Membr. Sci.* **1994**, *94*, 313.
19. Li, J.; Wang, S.; Nagaib, K.; Nakagawab, T.; Mau, A. H. *J. Membr. Sci.* **1998**, *138*, 143.
20. Liu, C.; Wilson, S. T.; Kulprathipanja, S. (to Honeywell UOP). U.S. Pat. 20090299015 (**2010**).
21. Scholes, A. C.; Kentish, S. E.; Stevens, G. W. *Rec. Pat. Chem. Eng.* **2008**, *1*, 52.
22. Minhas, F. T.; Memon, S.; Bhanger, M. I. *J. Incl. Phenom. Macrocycl. Chem.* **2010**, *67*, 295.
23. Qazi, M. A.; Qureshi, I.; Memon, S. *J. Fluoresc.* **2011**, *21*, 1231.
24. Minhas, F. T.; Qureshi, I.; Memon, S.; Bhanger, M. I. *Sep. Sci. Tech.* **2011**, *46*, 2400.
25. Minhas, F. T.; Memon, S.; Bhanger, M. I. *J. Macromol. Sci. Pure Appl. Chem.* **2013**, *50*, 215.
26. Rouis, A.; Mlika, R.; Dridi, C.; Davenas, J.; Ouada, H. B.; Halouani, H.; Bonnamour, I.; Jaffrezic, N. *Mater. Sci. Eng. C* **2006**, *26*, 247.
27. Thallapally, P. K.; Kirby, K. A.; Atwood, J. L. *New J. Chem.* **2007**, *31*, 628.
28. Atwood, J. L.; Barbour, L. J.; Thallapally, P. K.; Wirsig, T. B. *Chem. Commun.* **2005**, *51*.
29. Sliwa, W.; Kozlowski, C. Calixarene and Resorcinarenes; Wiley: Hoboken, NJ, **2009**.
30. Tsue, H.; Takahashi, H.; Ishibashi, K.; Inoue, R.; Shimizu, S.; Takahashi, D.; Tamura, R. *Cryst. Eng. Commun.* **2012**, *14*, 1021.
31. Atwood, J. L.; Barbour, L. J.; Jrga, A. *Angew. Chem. Int. Ed.* **2004**, *43*, 2948.
32. Lavrik, N. V.; Rossi, D. D.; Kazantseva, Z. I.; Nabok, A. V.; Nesterenko, B. A.; Piletsky, S. A.; Kalchenko, V. I.; Shivaniuk, A. N.; Markovskiy, L. N. *Nanotechnology* **1996**, *7*, 315.
33. Graham, B. F.; Harrowfield, J. M.; Tengrove, R. D.; Lagalante, A. F.; Bruno, T. J. *J. Inclusion Phenom. Macrocyclic Chem.* **2002**, *43*, 179.
34. Benosmane, N.; Guedioura, B.; Hamdi, S. M.; Hamdi, M.; Boutemeur, B. *Mater. Sci. Eng. C.* **2010**, *30*, 860.
35. Valente, A. J. M.; Jimenez, A.; Simoes, A. C.; Burrow, H. D.; Polishchuk, A. Y.; Lobo, V. M. M. *Eur. Polym. J.* **2007**, *43*, 2433.
36. Kaya, A.; Alpoguz, H. K.; Yilmaz, A. *Ind. Eng. Chem. Res.* **2013**, *52*, 5428.
37. Kim, J. S.; Yu, S. H.; Cho, M. H.; Shon, O. J.; Rim, J. A.; Yang, S. H.; Lee, J. K.; Lee, S. *J. Bull. Korean Chem. Soc.* **2001**, *22*, 519.
38. Aroon, M. A.; Ismail, A. F.; Matsuura, T.; Montazer-Rahmati, M. M. *Sep. Purif. Technol.* **2010**, *75*, 229.
39. Balagopal, N. N.; Keizer, K.; Elferink, W. J.; Gilde, M. J.; Verweij, H.; Burggraaf, A. J. *J. Membr. Sci.* **1996**, *116*, 161.
40. Dobre, T.; Pârvulescu, O. C.; Sanchez-Marcano, J.; Stoica, A.; Stroescu, M.; Iavorschi, G. *Sep. Purif. Technol.* **2011**, *82*, 202.
41. Teo, L. S.; Kuo, J. F.; Chen, C. Y. *J. Membr. Sci.* **1998**, *141*, 91.
42. Gutsche, C. D.; Nam, K. C. *J. Am. Chem. Soc.* **1988**, *110*, 6153.
43. Adams, R. T.; Lee, J. S.; Bae, T. H.; Ward, J. K.; Johnson, J. R.; Jones, C. W.; Nair, S.; Koros, W. J. *J. Membr. Sci.* **2011**, *367*, 197.
44. Shojaie, S. S.; Krantz, W. B.; Greenberg, A. R. *J. Membr. Sci.* **1994**, *94*, 281.
45. Qin, J. J.; Oo, M. H.; Cao, Y. M.; Lee, L. S. *Sep. Purif. Tech.* **2005**, *42*, 291.
46. Puleo, A. C.; Paul, D. R.; Kelley, S. S. *J. Membr. Sci.* **1989**, *47*, 301.
47. Pacheco, D. M.; Johnson, J. R.; Koros, W. *J. Ind. Eng. Chem. Res.* **2012**, *51*, 503.
48. Fischer, S.; Thummler, K.; Volkert, B.; Hettrich, K.; Schmidt, I.; Fischer, K. *Macromol. Symp.* **2008**, *262*, 89.
49. Arthanareeswaran. G.; Sriyamuna Devi, T. K.; Raajenthiren, M. *Sep. Purif. Technol.* **2008**, *64*, 38.
50. Zhang, A. Y.; Li, D. H.; Zhang, D. X.; Lu, H. B.; Xiao, H. Y. *J. Jia, Polym. Lett.* **2011**, *5*, 708.
51. Sijbesma, H.; Nymeijer, K.; Marwijk, R. V.; Heijboer, R.; Potreck, J.; Wessling, M. *J. Membr. Sci.* **2008**, *313*, 263.
52. Powell, C. E.; Qiao, G. G. *J. Membr. Sci.* **2006**, *279*, 1.